Geophysical Research Letters

RESEARCH LETTER
10.1029/2024GL111425

Seismic Reflection Imaging of Fluid-Filled Sills in the West Eifel Volcanic Field, Germany

Dario Eickhoff[1], Joachim R. R. Ritter[1], Felix Hloušek[2], and Stefan Buske[2]

[1]Karlsruhe Institute of Technology, Geophysical Institute, Karlsruhe, Germany, [2]TU Bergakademie Freiberg, Institute of Geophysics und Geoinformatics, Freiberg, Germany

Key Points:

- Quaternary volcanism in the Eifel region, Germany, still has active magmatic structures in the lower lithosphere
- Deep seismic reflection imaging reveals a rich inventory of sill-like structures beneath a volcanic field in the Eifel
- Reflections with negative-amplitude polarity from 15 km depth and the Moho are related to upwelling melts or fluids from the upper mantle

Supporting Information:

Supporting Information may be found in the online version of this article.

Correspondence to:

D. Eickhoff,
dario.eickhoff@kit.edu

Citation:

Eickhoff, D., Ritter, J. R. R., Hloušek, F., & Buske, S. (2024). Seismic reflection imaging of fluid-filled sills in the west eifel volcanic field, Germany. *Geophysical Research Letters*, *51*, e2024GL111425. https://doi.org/10.1029/2024GL111425

Received 23 JUL 2024
Accepted 21 OCT 2024

Abstract We applied state-of-the-art seismic processing and imaging techniques to crustal-scale seismic reflection data from the BELCORP/DEKORP87 lines 1A and 1B. The aim of the presented work was to identify structural evidence in the Earth's crust and upper mantle related to the ongoing magmatic activity in the Quaternary West Eifel Volcanic Field (WEVF) in Central Europe where ca. 70 eruptions happened since 65 ka. Following careful signal-processing, Fresnel volume migration was applied and yielded images with exceptionally strong lithospheric reflectors in the SE of the WEVF. Sparse signal representation revealed numerous reversed polarities. Using petrophysical relations, the corresponding reflections can be interpreted as reflections from melt and/or volatile-bearing (supercritical CO_2) zones which appear as horizontally elongated lens-shaped sills. Furthermore, we observed reflections with similarly inverted polarities from structural features located around the Moho at of 31 km depth, indicating fluids or melts from the uppermost mantle and supporting magmatic underplating models.

Plain Language Summary We re-processed a more than 35 years-old seismic dataset with new processing methods to search for active magmatic structures in the Earth's crust and upper mantle, Western Germany. There, in the Eifel mountains, volcanic eruptions happened until just 11,000 years ago. This young age, current volcanic gas emissions, current wide-spread uplift, and hints of magmatic processes at depth indicate that the volcanic processes are dormant but not extinct. A possible reawaking of volcanic eruptions would present a significant hazard in Central Europe, with the potential for severe impact on air traffic for example, The reprocessing of seismic data finds strongly reflecting structures at depths of 10–30 km beneath the youngest part of the West Eifel Volcanic Field. The observation of reversed signal amplitudes is a strong indication that some reflectors consist of magmatic melt, fluids, or gas. Thus, future hazard assessments should consider the presence of this magmatic material in the Earth's crust.

1. Introduction

In Central Europe, volcanic hazard does not seem to represent a significant threat. However, the most recent eruptions in Germany and France are of Holocene age (Global Volcanism Program, 2023). In the Eifel region of Germany (Figure 1), the history of volcanic eruptions (Nowell et al., 2006; Schmincke, 2007), ongoing gas emissions (Bräuer et al., 2013), and estimates of current melt in the upper mantle (Dahm et al., 2020; Ritter, 2007) do not indicate an end of the volcanic activity. One crucial point for risk assessment is the knowledge about active magmatic systems in the lithosphere. These are thought to be mush-like melt reservoirs in the form of sills, dykes etc (e.g., Sparks et al., 2019). Seismic imaging of melt in the lithosphere is quite challenging and its success depends on the volume, concentration, and type of melt distribution as well as the design of a seismological experiment (Paulatto et al., 2022). Melts, fluids, and volatiles reduce seismic velocity, especially for shear waves, and they increase anelastic damping and influence the ratio between compressional (P) and shear (S) wave velocities (*vp*/*vs*) (Mavko, 1980; Takei, 2017). In the Eifel region, Mechie et al. (1983) and Dahm et al. (2020) determined a strongly reduced P-wave velocity of approximately −20% underneath the Moho with seismic refraction data. They interpreted this seismic model as active magmatic underplating. Ritter (2007) described a low P- and S-wave velocity anomaly in the upper mantle, which can be explained by increased temperature and about 1% melt underneath the Eifel. Seismic reflections due to melt or fluid-bearing zones have not yet been observed in the Eifel but have been reported from other continental regions. The latter include sill-like structures in the US (Jarchow et al., 1993), Tibet (Brown et al., 1996), Campi Flegrei (Zollo et al., 2008) and the Eger Rift (Hrubková et al., 2017).

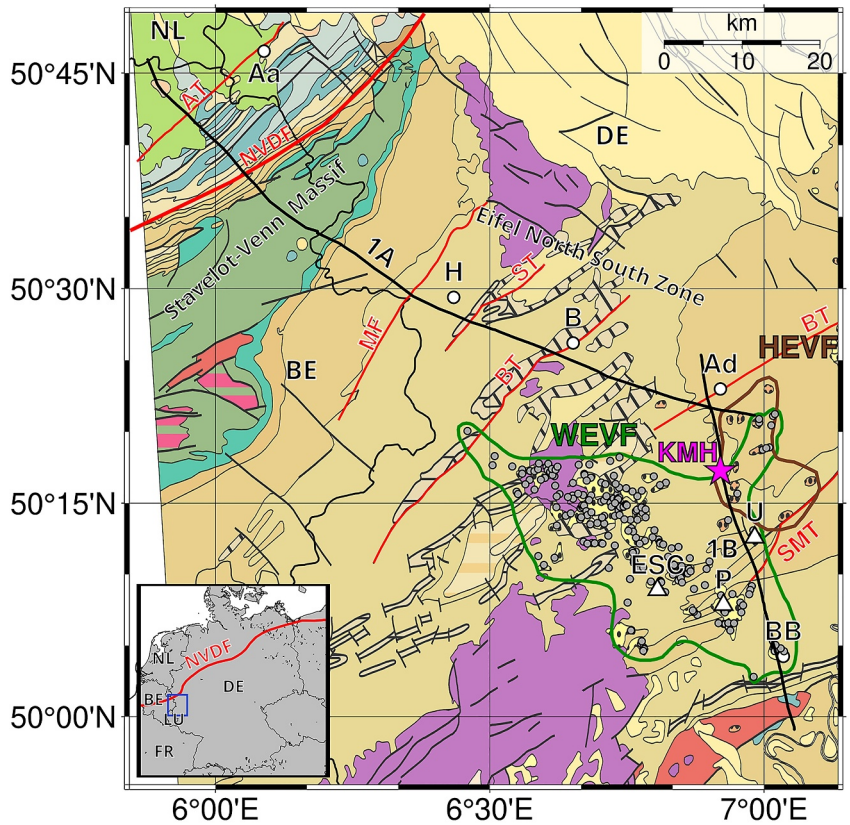

Figure 1. Geological map of the study area including the seismic lines BELCORP/DEKORP87 1A and 1B (black lines). The seismic lines are aligned about perpendicular to the local fault zones (red lines). Line 1 A runs NW-SE from the Aachen Thrust (AT) across the North Variscan Deformation Front (NVDF), the Stavelot-Venn Massif (SVM), the limestone troughs of the Eifel North-South Zone (ENSZ) and ends in the Tertiary Hoch Eifel Volcanic Field (HEVF). Line 1 B runs NNW to SSE across Line 1A in the HEVF, the Kelberg Magnetic High (KMH) and the SE area of West Eifel Volcanic Field (WEVF) with, for example, the Ulmener Maar (U), Pulvermaar (P), Emmelberg scoria cone (ESC), the Siegen Main Thrust (SMT) and the Bad Bertrich volcanic group (BB). Eruption centers are marked as gray circles. Aa: Aachen, Ad: Adenau B: Blankenheim, (h) Hellenthal. Background geology is from BGR (2020), the color code is shown in Figure S1 in Supporting Information S1. The inset map shows the position of the study area in the border region of Germany (DE) and Belgium (BE) with neighboring Luxemburg (LU), France (FR) and the Netherlands (NL).

Recently, Hensch et al. (2019) interpreted up to 45 km deep low-frequency (ca. 2–8 Hz) earthquakes as possible deep injections of magmatic fluids near the Laacher See Volcano in the East Eifel Volcanic Field. There, a strong eruption (volcanic explosivity index = 6) occurred only 13,000 years ago from which ashes can be found in several European countries (van den Bogaard and Schmincke, 1985). Around 30 km further to the west, in the WEVF, a series of approximately 70 eruptions (e.g., Dauner Maars, Pulvermaar, Wartgesberg and Bad Bertrich volcanic groups etc.) started only ca. 65,000 years ago (Figure 1 and Figure S5 in Supporting Information S1; Schmincke, 2007; Brandt & Ritter, 2023). The most recent eruption at the Ulmener Maar happened only 11,000 years ago and is still visible as a ca. 340 m wide crater.

The NE part of the WEVF overlaps with the much older Tertiary High Eifel Volcanic Field (HEVF), which was active at 44–39 Ma and 37–35 Ma (Fekiacova et al., 2007). The HEVF exhibits distinct geophysical signatures, including deep-reaching crustal anomalies, such as the Kelberg Magnetic High (KMH) as documented by Büchel (1992). This positive magnetic anomaly, with an estimated diameter of around 20 km, is thought to be associated with the Tertiary magma chamber located at a depth of ca. 10 km. At the KMH there is a seismically transparent zone which is completely different from reflective structures in the direct vicinity (Dahm et al., 2020; DEKORP Research Group et al., 1991).

2. Seismic Reflection Data

Seismic data were acquired in 1987 along long-range deep-reaching reflection lines within the German Continental Reflection Seismic Program (DEKORP) (In Meissner & Bortfeld, 1990; Stiller et al., 2020a, 2020b). The BELCORP—DEKORP line 1A covers the western part of the Variscan Rhenish Massif, extending from the Stavelot-Venn Massif (SVM) in Belgium in the west to the Eifel Mountains in Germany in the east. It runs south of the city of Aachen across the Eifel Mountains and ends near the town Adenau in the Tertiary HEVF (Figure 1). Line 1 B starts NW of Adenau and runs SSE across the HEVF, over the KMH, and further across the Quaternary WEVF to terminate close to the Moselle River (Figure 1 and Figure S5 in Supporting Information S1). To the south an additional seismic line 1C is located, which has not been reprocessed within this work but is described in DEKORP Research Group et al. (1991) and Dahm et al. (2020). The DEKORP seismic lines provide a unique dataset to explore the deep structure beneath Germany and its diverse tectonic units.

The dataset was acquired with five Vibroseis trucks weighing 19.4 *t* each that generated a linear sweep from 12 to 48 Hz with a peak force of 125 kN and a duration of 20 s at 40 m source distances and five-fold vertical stacking. An additional 16 s of listening time allowed for the recording of near-vertical reflection signals from the lower lithosphere (ca. 50 km depth). Up to 400 geophones were deployed at 40 m distances in an asymmetric split-spread geometry, with a total line length of 16 km. A total of 1,891 and 1,049 vibration points were used for lines 1A and 1B, respectively (Stiller, M., 2020a, 2020b), which leads to an up to 200-fold coverage. Further details can be found in the supplementary materials.

3. Imaging Results

The results of conventional CMP processing are published in DEKORP Research Group et al. (1991), while an updated processing result including common-reflection-surface (CRS) stacking is discussed in Dahm et al. (2020). Here, we conducted a standard seismic time-domain pre-processing for both lines (with processing steps shown in the workflow in Figure S4 in Supporting Information S1), which enhances the amplitudes of reflection phases while attenuating noise and undesired first-arrival phases. The performance of the pre-processing is shown in Figure S5 in Supporting Information S1. Subsequently, Fresnel volume migration (FVM, Buske et al., 2009) was applied to precisely image reflecting structures at depth. Velocity models derived from the analysis of local seismicity (Ritter et al., 2024) were used as input for the FVM. Additionally, a comprehensive amplitude polarity analysis was conducted to determine the nature of the impedance contrasts at the reflectors. This has been combined with a sparse signal deconvolution technique to separate overlapping signals (Dai et al., 2018). A comprehensive description of the analyzed reflectors is provided in the supplementary Information.

4. Seismic Reflectors and Their Origin

4.1. Overview

The migration results for lines 1A and 1B reveal a rich inventory of reflectors from the surface down to the uppermost mantle (Figures 2 and 3). Some reflectors are well resolved for the first time and many new details (relative reflection strength and impedance contrast) are found. Many near-surface structures can be identified and correlated with the known geology and previously imaged reflectors (DEKORP Research Group et al., 1991), for example, we observe shallow reflectors related to the NVDF (Figure 2): Aachen Thrust (1, 2, 3, 4), Sötenich Thrust (5), and Blankenheim Thrust (6) with unprecedented resolution.

The upper crust down to about 15 km depth is characterized by several distinct reflectors, with varying dip directions (1–6 in Figure 2; 13, 14 and 18 in Figure 3). Along line 1A, the reflectors dip approximately SE in the upper part of the lower crust (ca. 15–22 km depth), whereas at greater depths the reflectors appear subhorizontal or dip preferentially toward NW (11 and 12 in Figure 2). The deep crustal reflectors form an often described lower-crustal laminated structure (Mooney & Meissner, 1992) along both lines with the exception at a non-reflective zone below the HEVF (17 in Figure 3).

The lower end of the visible reflectors indicates the crust-mantle transition (Moho) (7–10 in Figures 2 and 20 in Figure 3). The Moho is nearly horizontal below the NW part of line 1A (Figure 2) with a minimal dip toward the SE with its maximum depth at around 31 km below the Blankenheim area. Further SE the Moho rises toward the

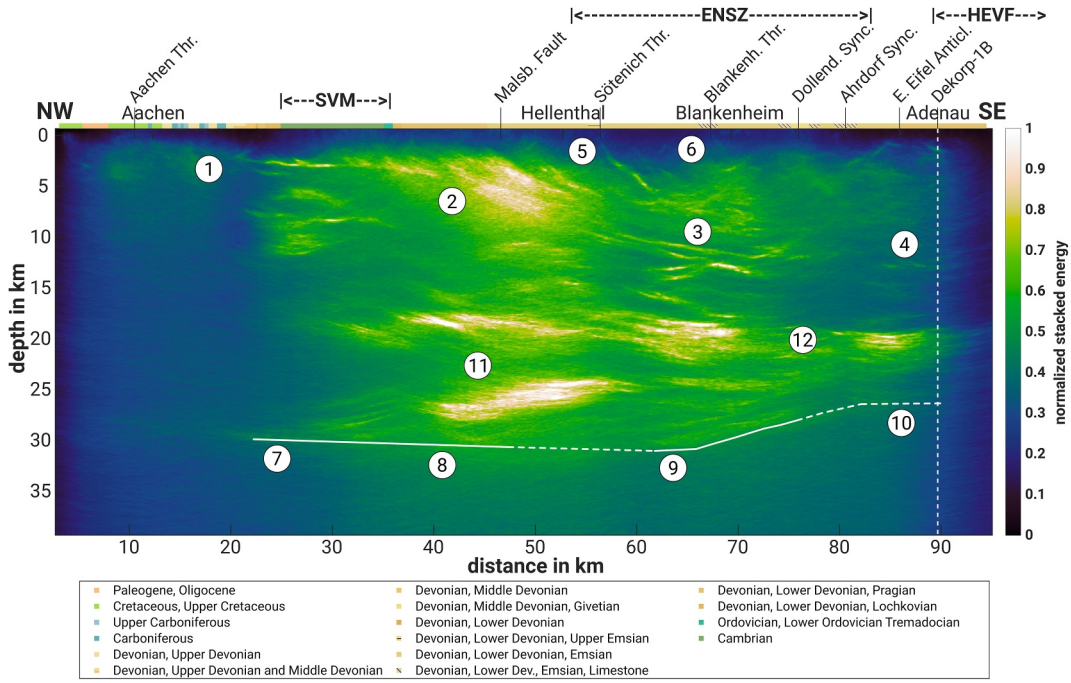

Figure 2. FVM result along line 1A (Figure 1) with normalized stacked energy as amplitude value. Individual reflective elements are numbered, see also detailed description in the supplementary information. Our interpreted Moho is shown as solid line, connected, and extrapolated to the SE by dashed lines where its location appears unclear. ENSZ: Eifel North South Zone, HEVF: Hoch Eifel Volcanic Field, SVM: Stavelot Venn Massif.

HEVF (Adenau region) to about 26 km depth. Along line 1B (Figure 3), the Moho dips toward SSE (profile kilometers 0–35) and subsequently rises toward the SSE end of the line.

4.2. HEVF

Below the north of the HEVF at the crossing of lines 1A and 1B, three clear reflectors (14–16) can be observed which dip SSE (Figure 3). Reflector 14 corresponds to reflector 4 in Figure 2 and is part of the NVDF main detachment. In the lower crust, the prominent reflector 15 represents the top of a reflective sequence extending down to reflector 16 at the Moho. This sequence is also observed along line 1A and it is possibly composed of sills which may be of either recent (WEVF), Tertiary (HEVF) or Permian age (Shaw, 2021). The main feature of the HEVF is the seismically transparent zone (STZ) (17 in Figure 3; Figure S7 in Supporting Information S1) located below the Tertiary Hochkelberg Volcano with the KMH at profile kilometers 12–27. This zone is also described in DEKORP Research Group et al. (1991), Büchel (1992), and Dahm et al. (2020). The lack of reflections in the STZ remains unclear. Büchel (1992) proposed incoherent scattering of the downgoing seismic wavefield at small-scale fractures inside a Tertiary magmatic intrusion zone. The high resolution of our reprocessed data limits this fracture model to small cracks, with lengths of less than 300 m, assuming a dominant frequency of 20 Hz and/or extremely low-impedance contrasts. Otherwise, distinct reflections should be visible.

Dahm et al. (2020) proposed that the STZ is potentially due to a hot mush zone north of the Siegen Main Thrust (SMT) and bounded by a steep Moho step. This interpretation implies that the STZ is related to the WEVF magmatism. However, the majority of the most recent eruptions in the WEVF along line 1B occurred south of the STZ (e.g., Mertz et al., 2015) and our image (Figure 3, Figure S7 in Supporting Information S1) can be interpreted without a steep Moho step.

Atop the STZ a strongly reflecting zone (18 in Figure 3) is interpreted by Büchel (1992) as an upward volatile magmatic flow or a cap-rock-like magmatic layer related to the magma reservoir of the HEVF. Dahm et al. (2020) describe this bright spot as a possible layer structure with CO_2- and/or fluid-bearing layers below solidified sills of a Tertiary magma reservoir. In subsection K (Figure S20 in Supporting Information S1), the bright spot has a depth extension of 8–10 km between profile kilometers 17.5 to 21.5. The lateral coherence of reflection signals

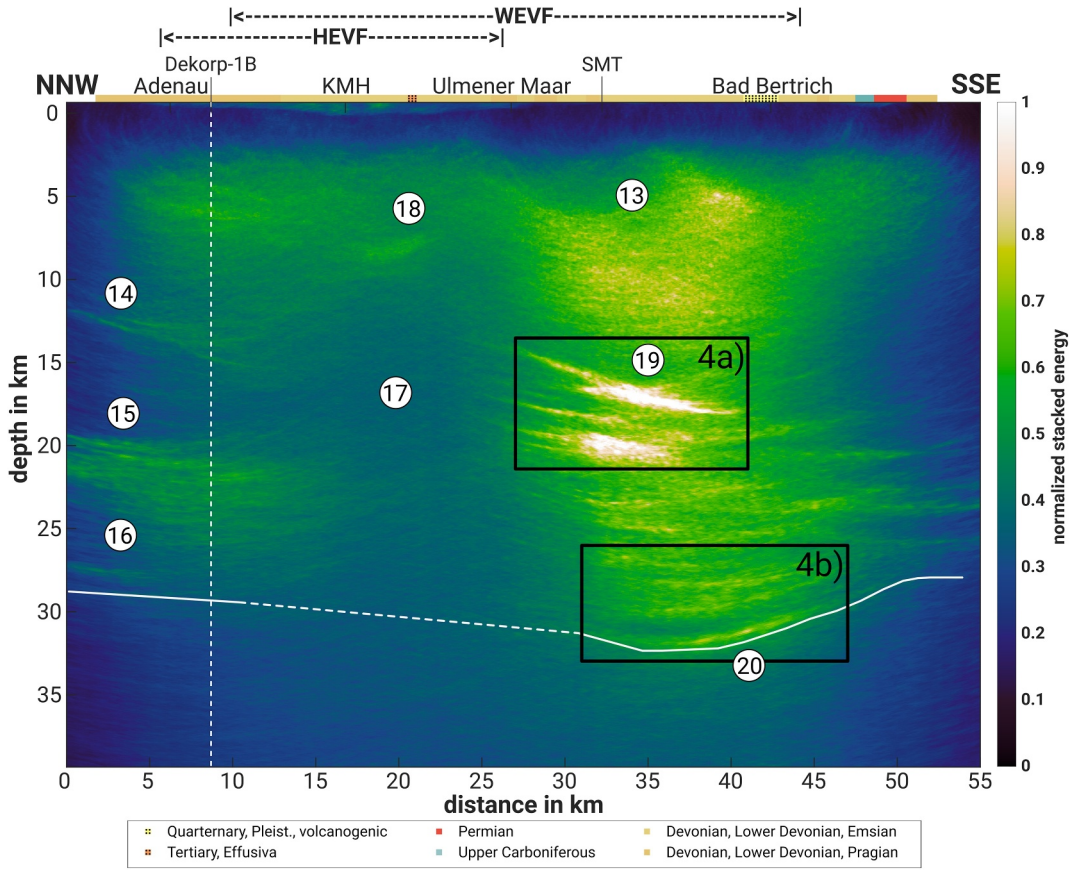

Figure 3. FVM result along line 1B (Figure 1) with normalized stacked energy as amplitude value and the interpreted Moho. HEVF: Hoch Eifel Volcanic Field, WEVF: West Eifel Volcanic Field. The black boxes outline the locations of reflection phases shown in Figures 4a and 4b.

with the same polarity is mostly short, less than a few hundred meters. The occurrence of negative impedance contrasts may support the presence of fluids, however clear, continuous solid barriers cannot be resolved (Figure S20 in Supporting Information S1).

4.3. WEVF

The southeastern half of line 1B crosses the dormant WEFV with the volcanic centers Jungfernweiher Maar, Ulmener Maar (most recent eruption ca. 10.9 ka), Pulvermaar Region (a ca. 700 m wide crater, ca. 21 ka, Zöller and Blanchard, 2009), Wartgesberg (ca. 33 ka, Schmidt et al., 2017) and Bad Bertrich (ca. 15–17 ka) volcanic groups. Here the strongest reflections are observed along line 1B (Figure 3 and Figure S7 in Supporting Information S1). An inclined reflective zone (13 in Figure 3) coincides with the surface trace of the SMT. In Figure S23 in Supporting Information S1, numerous short high-amplitude reflections with negative polarity are evident within this zone, extending only across a few hundred meters along the geophone spread. The SMT and its tectonic history may have formed a 2–3 km wide damage zone and fault gauge with crushed rock and increased porosity, that allowed the intrusion and storage of magmatic fluids, imaged as negative reflections. This magmatic reservoir possibly fed the numerous Pleistocene volcanic eruptions. At profile kilometers 27–41, the most coherent reflector (19) is located at 14.5–17.5 km depth. It represents the top of a clear reflector series that extends to the Moho (20). Figure 4a depicts reflector 19 in greater detail including enhanced signal polarities (23I–25I). In order to determine the lateral dimensions of the smallest resolvable structures down to the Moho, a resolution analysis was carried out. For this we placed six point diffractors at a depth of 31.4 km and performed FVM with synthetic seismograms. Based on these tests, the smallest resolvable size of typical impedance is 300 ± 50 m (Text S6 in Supporting Information S1, Figure S25 in Supporting Information S1). Smaller structures may be present but cannot be resolved with our method. The images in Figure 4 contain several patches with reversed

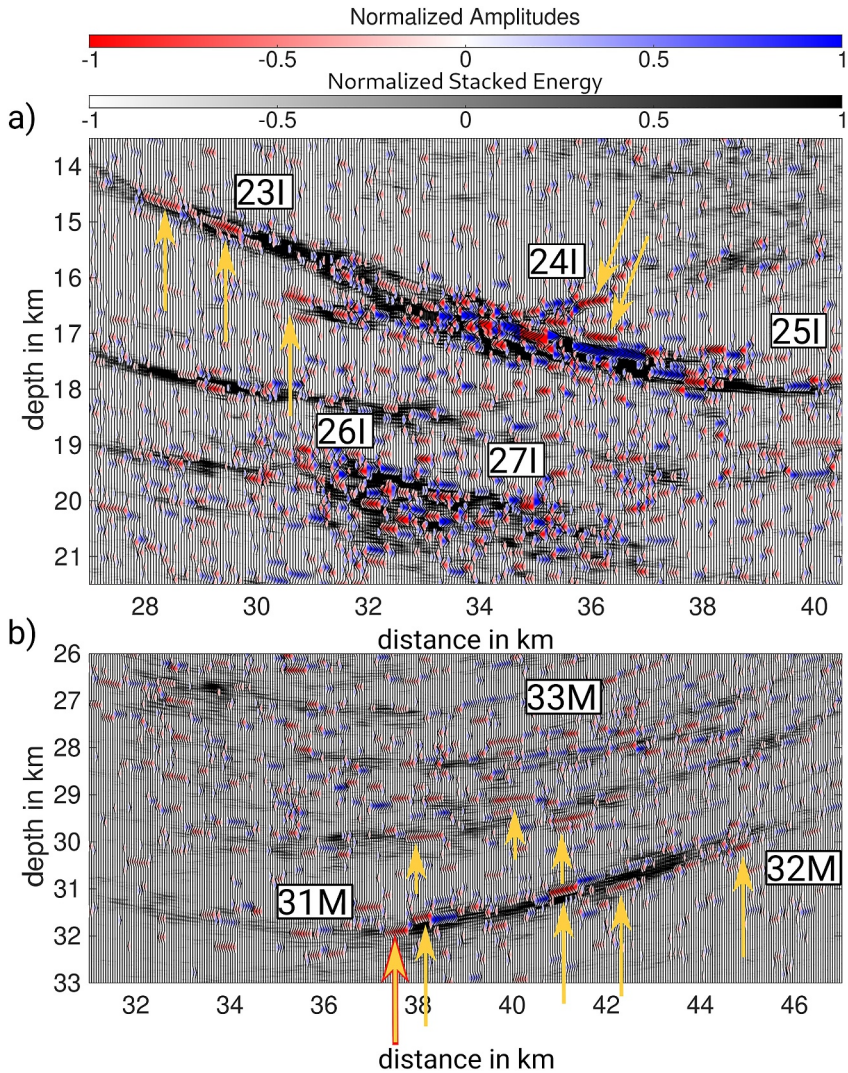

Figure 4. Seismic images with sparse representation of the polarity of the seismic phases. (a) subsection I, (b) subsection M from line 1B (see black boxes Figure 3 for location). Blue fillings indicate positive-polarity phases, hence the same polarity as the input signal. Red fillings indicate negative-polarity reflections due to a low-impedance contrast of the corresponding reflector. The yellow arrows mark distinct negative-polarity patches.

polarity across neighboring traces, for example, at the upper ends of reflectors 23I and 24I in the lower crust and at 31 and 32M close to the Moho (yellow arrows in Figure 4). Their lengths of 300–500 m are within the resolution of the FVM (Figure S25 in Supporting Information S1).

The deeper reflectors 26I and 27I also contain laterally coherent negative and positive polarity patches. These sill-like reflectors occur across the whole lower crust and end at the prominent reflector 20 (Figure 3), highlighted in Figure 4b with reflectors 31–33M at the Moho. In Figure 5, we compare the observed and modeled reflection signal for the sequence of the impedance contrasts above the Moho (M31, red outlined arrow in Figure 4b). The convolution of the input signal with reflection coefficients of up to −0.11 (Section 4.4, Figure 5), match the observed signal well.

4.4. Petrophysical Interpretation

The petrophysical properties of the impedance contrasts are estimated from the reflection coefficients. The two-way amplitude A_1 of the reflected signal is approximately equal to (neglecting geometrical spreading):

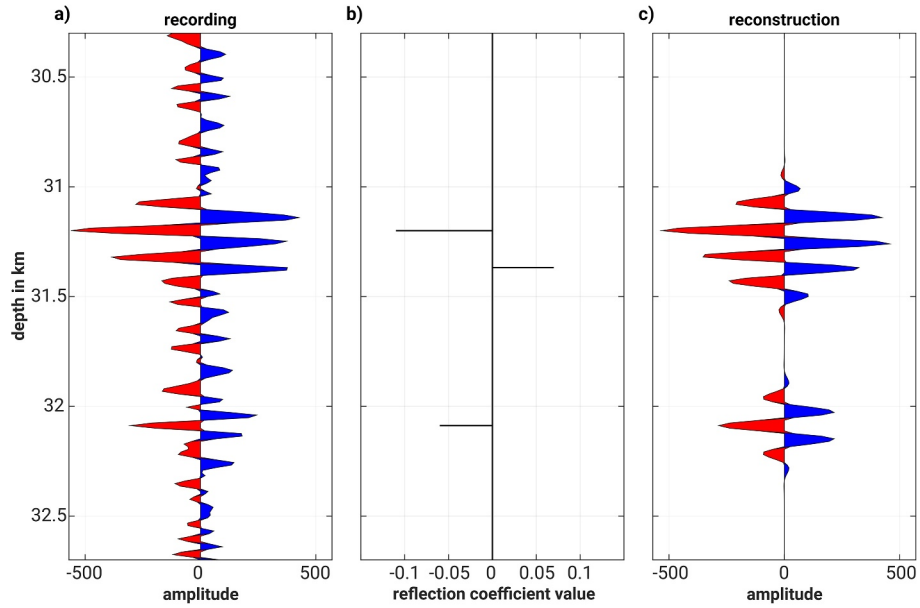

Figure 5. Modeling of seismic reflection signal at reflector 31M (orange arrow in Figure 4). (a) Observed signal, (b) reflection coefficient in 30.3–32.7 km depth with a series of positive and negative polarity contrasts, (c) reconstructed synthetic signal. The reconstruction uses a tapered and smoothed Klauder wavelet, which represents the autocorrelation function of a Vibroseis sweep.

$$A_1 = A_0 \exp^{\left(\frac{-\pi f t}{Q}\right)} \tag{1}$$

A_0, Q, f, and t are the initial source amplitude, seismic quality factor, center frequency of the signal, and two-way travel-time. The measured amplitude of the reflected signal, A_r, depends on the reflection coefficient R:

$$R = \frac{A_r}{A_0} \tag{2}$$

To roughly estimate the reflection coefficients at depth the amplitudes A_0 and A_r are measured in a raw seismic shot record. A_0 is the average first-arrival amplitude and A_r is measured at the respective reflection signal. These amplitudes are only corrected for geometrical spreading and Q is taken as 250, as an average value in the Earth's crust (Sheehan et al., 2014). With (1) and (2), and assuming the zero-offset vertical incidence case, we find an estimated maximum reflection coefficient of $R = -0.11$ (Figure 5), corresponding to a P-wave velocity (vp) change (δvp) of ca. -20%. Both values have an uncertainty of ca. 20%, so $R = -0.11 \pm 0.3$ and $\delta vp = -20\% \pm 4\%$. This reduction may be due to reduced density, vp and/or a fluid phase associated with the reflector. While this estimation remains greatly simplified, it still provides a reasonable δvp for reflector 31M and similar reflectors along line 1B.

The middle and lower crust of the Eifel region is composed of meta-sediments, meta-granitoids and mafic granulites (Mengel et al., 1991; Sachs & Hansteen, 2000) with P-wave velocities in the range of ca. 6.3–6.5 km/s. A massive solid layer with $\delta vp \sim -20\%$ ($vp \sim 5.0$–5.2 km/s) is not realistic, as rock material at 10–30 km depth is typically characterized by higher vp (Christensen & Mooney, 1995). However, fluids (e.g., supercritical CO_2) or melt can cause a strong negative δvp, depending on its type of distribution within the rock matrix. We us the code *compute_seismic_properties_magma.m* by Carrara et al. (2022, supplement) to compute vp of a rock material with up to three different phases (solid, fluid and gas). Ambient pressure and temperature in the Eifel and rock physic parameters of are taken from the literature (see Supporting Information S1). A δvp of $-20\% \pm 4\%$, can be explained with an accumulation of 5%–10% basaltic melt (fluid phase) of or 1.5%–3.3% supercritical CO_2 in the lower crust. In the Moho region, similar values of 5%–10% basaltic melt or 2.3%–4.8% CO_2 can produced the required δvp for the reflection signals. A gas phase of just 1% leads to an unrealistic low vp (ca. -70% reduction)

and at the ambient *p-T* conditions a supercritical state of magmatic volatiles is more realistic (Edmonds et al., 2020).

Our estimated melt ranges are in agreement with studies in other regions studied with seismological methods (Chu et al., 2010; Jarchow et al., 1993; Schmandt et al., 2019) and are in accordance with recent petrophysical models relating melt and seismic velocity in magmatic settings (Caricchi et al., 2008; Lyakhovsky et al., 2021; Ueki and Iwamori, 2016).

The positive amplitude reflections observed in the lower crust can be explained by the presence of solidified pyroxenitic intrusions (Shaw, 2024) that have a $\delta vp \sim +15\%$ to $+20\%$ relative to the mafic granulite matrix (Christensen & Mooney, 1995).

5. Conclusions

The reprocessing of BELCORP/DEKORP87 lines 1A and 1B reveals distinct and well resolved images of the crustal structure in the western Eifel region, along with information on amplitude polarities for petrophysical interpretation. The observed negative impedance contrasts can be explained by patches of magmatic fluids or partial melt of up to 10% in sills underneath the WEVF. This suggests that this Pleistocene volcanic field is presently in a dormant state and that new eruptions could occur once the melt has enough buoyancy to rise to the surface. Although 10% basaltic melt is a low value, this equates to a volume of about 50 million cubic meters of melt for just one sill which is approximately 6 km long, 200 m thick (Figure 4) and possibly 500 m wide. A part of this volume (2%–5%) could be filled with supercritical CO_2 that is found in numerous springs (e.g., Bräuer et al., 2013; May et al., 1996) and that is even commercially exploited in the Eifel region.

Compared to other Quaternary intraplate volcanic fields in Europe such as the Eger Rift (Hrubcová et al., 2017), Ciomadual volcanic complex (Laumonier et al., 2019) or Chaînes des Puys (France et al., 2016), evidence for ongoing deep magmatic activity is well documented in the Eifel by passive and active seismic methods (Ritter, 2007; Hensch et al., 2019; Dahm et al., 2020; this study). Herewith our seismic image of a section of the WEVF indicates melt/fluid pockets and deep low-frequency seismicity is documented in the EEVF (Hensch et al., 2019). Consequently, high-resolution studies utilizing modern geophysical and geochemical methodologies should be conducted in order to obtain more comprehensive constraints in both volcanic fields for a state-of-the-art volcanic assessment, following for example, Ewert et al. (2018).

Data Availability Statement

The DEKORP87–1A and DEKORP87–1B data used for seismic reflection imaging in the study are available Stiller et al. (2020a, 2020b).

Acknowledgments
We thank Cliff Shaw and one anonymous reviewer for their helpful reviews and valuable feedback. We also thank GFZ Data Services for providing access to the seismic datasets of the DEKORP87–1A and –1B lines used in this study. Open Access funding enabled and organized by Projekt DEAL.

References

Brandt, A., & Ritter, J. (2023). A new database of eruptions in the Quaternary Eifel Volcanic Fields, Germany, for the spatial, temporal and statistical description of the volcanism. *9th Physics of Volcanoes, Abstracts, Hannover*, *10*.

Bräuer, K., Kämpf, H., Niedermann, S., & Strauch, G. (2013). Indications for the existence of different magmatic reservoirs beneath the Eifel area (Germany): A multi-isotope (C, N, He, Ne, Ar) approach. *Chemical Geology*, *356*, 193–208. https://doi.org/10.1016/j.chemgeo.2013.08.013

Brown, L. D., Zhao, W., Nelson, K. D., Hauck, M., Alsdorf, D., Ross, A., et al. (1996). Bright spots, structure, and magmatism in southern Tibet from INDEPTH seismic reflection profiling. *Science*, *274*(5293), 1688–1690. https://doi.org/10.1126/science.274.5293.1684

Büchel, G. (1992). Das Kelberger Hoch. Tiefenstruktur und Geodynamik einer magnetischen Anomalie in der Eifel. *Geowissenschaften*, *10*(5), 132–142.

Bundesanstalt für Geowissenschaften und Rohstoffe (BGR). (2020). *INSPIRE: The General Geological Map of the Federal Republic of Germany 1:250000 (GÜK250)*. Retrieved from https://www.geoportal.de/Metadata/f9ca7f17-90b4-43e3-9f9c-15472ea7ab8d

Buske, S., Gutjahr, S., & Sick, C. (2009). Fresnel volume migration of single-component seismic data. *Geophysics*, *74*(6), WCA47–WCA55. https://doi.org/10.1190/1.3223187

Caricchi, L., Burlini, L., & Ulmer, P. (2008). Propagation of P and S-waves in magmas with different crystal contents: Insights into the crystallinity of magmatic reservoirs. *Journal of Volcanology and Geothermal Research*, *178*(4), 740–750. https://doi.org/10.1016/j.jvolgeores.2008.09.006

Carrara, A., Lesage, P., Burgisser, A., Annen, A., & Bergantz, G. W. (2022). The dispersive velocity of compressional waves in magmatic suspensions. *Geophysical Journal International*, *228*(3), 2122–2136. https://doi.org/10.1093/gji/ggab432

Christensen, N. I., & Mooney, W. D. (1995). Seismic velocity structure and composition of the continental crust: A global view. *Journal of Geophysical Research*, *100*(B6), 9761–9788. https://doi.org/10.1029/95jb00259

Chu, R., Helmberger, D. V., Sun, D., Jackson, J. M., & Zhu, L. (2010). Mushy magma beneath yellowstone. *Geophysical Research Letters*, *37*(1), L01306. https://doi.org/10.1029/2009GL041656

Dahm, T., Stiller, M., Mechie, J., Heimann, S., Hensch, M., Woith, H., et al. (2020). Seismological and geophysical signatures of the deep crustal magma systems of the Cenozoic volcanic fields beneath the Eifel, Germany. *Geochemistry, Geophysics, Geosystems*, *21*(9), e2020GC009062. https://doi.org/10.1029/2020GC009062

Dai, R., Yin, C., Yang, S., & Zhang, F. (2018). Seismic deconvolution and inversion with erratic data. *Geophysical Prospecting*, *66*(9), 1684–1701. https://doi.org/10.1111/1365-2478.12689

DEKORP Research Group, Anderle, H. J., Bittner, R., Bortfeld, R., Bouckaert, J., Büchel, G., et al. (1991). Results of the DEKORP 1 (BEL-CORP-DEKORP) deep seismic reflection studies in the western part of the Rhenish Massif. *Geophysical Journal International*, *106*(1), 203–227. https://doi.org/10.1111/j.1365-246X.1991.tb04612.x

Edmonds, M., Tutolo, B., Iacovino, K., & Moussallam, Y. (2020). Magmatic carbon outgassing and uptake of CO_2 by alkaline waters. *American Mineralogist*, *105*(1), 28–34. https://doi.org/10.2138/am-2020-6986CCBY

Ewert, J. W., Diefenbach, A. K., & Ramsey, D. W. (2018). 2018 update to the U.S. Geological Survey national volcanic threat assessment. *U.S. Geological Survey Scientific Investigations Report*, *2018–5140*, 40. https://doi.org/10.3133/sir20185140

Fekiacova, Z., Mertz, D. F., & Hofmann, A. W. (2007). Geodynamic setting of the tertiary hocheifel volcanism (Germany), part II: Geochemistry and Sr, Nd and Pb isotopic compositions. In J. R. R. Ritter & U. R. Christensen (Eds.), *Mantle plumes - a multidisciplinary approach* (pp. 207–238). Springer Verlag.

France, L., Demacon, M., Gurenko, A. A., & Briot, D. (2016). Oxygen isotopes reveal crustal contamination and a large, still partially molten magma chamber in Chaîne des Puys (French Massif Central). *Lithos*, *260*, 28–338. https://doi.org/10.1016/j.lithos.2016.05.013

Global Volcanism Program. (2023). *Volcanoes of the world (database v. 5.1.1; 17 aug 2023). Distributed by* smithsonian institution*, compiled by venzke*. E. https://doi.org/10.5479/si.GVP.VOTW5-2023.5.1

Hensch, M., Dahm, T., Ritter, J., Heimann, S., Schmidt, B., Stange, S., & Lehmann, K. (2019). Deep low-frequency earthquakes reveal ongoing magmatic recharge beneath Laacher See Volcano (Eifel, Germany). *Geophysical Journal International*, *216*(3), 2025–2036. https://doi.org/10.1093/gji/ggy532

Hrubcová, P., Geissler, W. H., Bräuer, K., Vavryčuk, V., Tomek, Č., & Kämpf, H. (2017). Active magmatic underplating in western Eger Rift, central Europe. *Tectonics*, *36*(12), 2846–2862. https://doi.org/10.1002/2017TC004710

Jarchow, C. M., Thompson, G. A., Catchings, R. D., & Mooney, W. D. (1993). Seismic evidence for active magmatic underplating beneath the basin and range province, western United States. *Journal of Geophysical Research*, *98*(12), 22095–22108. https://doi.org/10.1029/93jb02021

Laumonier, M., Karakas, O., Bachmann, O., Gaillard, F., Lukacs, R., Seghedi, I., et al. (2019). Evidence for a persistent magma reservoir with large melt content beneath an apparently extinct volcano. *Earth and Planetary Science Letters*, *521*, 79–90. https://doi.org/10.1016/j.epsl.2019.06.004

Lyakhovsky, V., Shalev, E., Kurzon, I., Zhu, W., Montesi, L., & Shapiro, N. M. (2021). Effective seismic wave velocities and attenuation in partially molten rocks. *Earth and Planetary Science Letters*, *572*, 117117. https://doi.org/10.1016/j.epsl.2021.117117

Mavko, G. M. (1980). Velocity and attenuation in partially molten rocks. *Journal of Geophysical Research*, *85*(B10), 5173–5189. https://doi.org/10.1029/JB085iB10p05173

May, F., Hoernes, S., & Neugebauer, H. (1996). Genesis and distribution of mineral waters as a consequence of recent lithospheric dynamics: The Rhenish Massif, Central Europe. *Geologische Rundschau*, *85*(4), 782–799. https://doi.org/10.1007/BF02440111

Mechie, J., Prodehl, C., & Fuchs, K. (1983). The long-range seismic refraction experiment in the rhenish Massif. In *Plateau uplift* (pp. 260–275). Springer.

Meissner, R. & Bortfeld, R. K. (Eds.) (1990)., *DEKORP atlas, results of deutsches kontinentales reflexionsseismisches programm* (p. 19). Springer-Verlag. + 80 seismic sections. https://doi.org/10.1007/978-3-642-75662-7

Mengel, K., Sachs, P. M., Stosch, H. G., Wörner, G., & Loock, G. (1991). Crustal xenoliths from Cenozoic volcanic fields of West Germany: Implications for structure and composition of the continental crust. *Tectonophysics*, *195*(2–4), 271–289. https://doi.org/10.1016/0040-1951(91)90215-e

Mertz, D. F., Löhnertz, W., Nomade, S., Pereira, A., Prelević, D., & Renne, P. R. (2015). Temporal–spatial evolution of low-SiO_2 volcanism in the Pleistocene West Eifel volcanic field (West Germany) and relationship to upwelling asthenosphere. *Journal of Geodynamics*, *88*, 59–79. https://doi.org/10.1016/j.jog.2015.04.002

Mooney, W. D., & Meissner, R. (1992). Multi-genetic origin of crustal reflectivity: A review of seismic reflection profiling of the continental lower crust and Moho. In D. M. Fountain, R. Arculus, & R. W. Kay (Eds.), *Continental lower crust* (pp. 45–79). Elsevier.

Nowell, D. A. G., Jones, M. C., & Pyle, D. M. (2006). Episodic quaternary volcanism in France and Germany. *Journal of Quaternary Science*, *21*(6), 645–675. https://doi.org/10.1002/jqs.1005

Paulatto, M., Hooft, E. E., Chrapkiewicz, K., Heath, B., Toomey, D. R., & Morgan, J. V. (2022). Advances in seismic imaging of magma and crystal mush. *Frontiers in Earth Science*, *10*. https://doi.org/10.3389/feart.2022.970131

Ritter, J., Koushesh, K., Schmidt, B., Föst, J.-P., Bühler, J., Hensch, M., & Mader, S. (2024). Seismological monitoring of magmatic and tectonic earthquakes in the East Eifel volcanic field. *Journal of Seismology*. https://doi.org/10.1007/s10950-024-10257-w

Ritter, J. R. R. (2007). The seismic signature of the Eifel plume. In J. R. R. Ritter & U. R. Christensen (Eds.), *Mantle plumes - a multidisciplinary approach* (pp. 379–404). Springer Verlag.

Sachs, P., & Hansteen, T. H. (2000). Pleistocene underplating and metasomatism of the lower continental crust: A xenolith study. *Journal of Petrology*, *41*(3), 331–356. https://doi.org/10.1093/petrology/41.3.331

Schmandt, B., Jiang, C., & Farrell, J. (2019). Seismic perspectives from the western U.S. on magma reservoirs underlying large silicic calderas. *Journal of Volcanology and Geothermal Research*, *384*, 158–178. https://doi.org/10.1016/j.jvolgeores.2019.07.015

Schmidt, C., Schaarschmidt, M., Kolb, T., Büchel, G., Richter, D., & Zöller, L. (2017). Luminescence dating of late Pleistocene eruptions in the Eifel volcanic field, Germany. *Journal of Quaternary Science*, *32*(5), 628–638. https://doi.org/10.1002/jqs.2961

Schmincke, H. U. (2007). The quaternary volcanic field of the East and West Eifel (Germany). In J. R. R. Ritter & U. R. Christensen (Eds.), *Mantle plumes - a multidisciplinary approach* (pp. 241–322). Springer.

Shaw, C. S. J. (2021). New evidence for upper Permian crustal growth below Eifel, Germany, from mafic granulite xenoliths. *European Journal of Mineralogy*, *33*(2), 233–247. https://doi.org/10.5194/ejm-33-233-2021

Shaw, C. S. J. (2024). Clinopyroxenite xenoliths record magma transport and crystallization in the middle and upper crust: A case study from the rockeskyllerkopf volcanic complex, West Eifel, Germany. *Journal of Petrology*, *65*(4), egae035. https://doi.org/10.1093/petrology/egae035

Sheehan, A. F., de la Torre, T. L., Monsalve, G., Abers, G. A., & Hacker, B. R. (2014). Physical state of Himalayan crust and uppermost mantle: Constraints from seismic attenuation and velocity tomography. *Journal of Geophysical Research: Solid Earth*, *119*(1), 567–580. https://doi.org/10.1002/2013jb010601

Sparks, R. S. J., Annen, C., Blundy, J. D., Cashman, K. V., Rust, A. C., & Jackson, M. D. (2019). Formation and dynamics of magma reservoirs. *Philosophical Transactions from the Royal Society A*, *377*(2139), 0019. https://doi.org/10.1098/rsta.2018.0019

Stiller, M. (2020a). Technical Report Profile DEKORP 1987-1A with original technical PHX and SEGY format descriptions and applied transcription rules. Retrieved from https://gfzpublic.gfz-potsdam.de/pubman/item/item_5006750

Stiller, M. (2020b). Technical Report Profile DEKORP 1987-1B with original technical PHX and SEGY format descriptions and applied transcription rules. https://gfzpublic.gfz-potsdam.de/pubman/item/item_5006752

Stiller, M., Kaerger, L., Agafonova, T., Krawczyk, C., Oncken, O., & Weber, M., & Former DEKORP Project Leaders, Former DEKORP/BELCORP Research Group, Former DEKORP Processing Centre. (2020a). Deep seismic reflection profile DEKORP 1987-1A across the western Rhenish Massif, West Germany/East Belgium. *GFZ Data Services*. [dataset]. https://doi.org/10.5880/GFZ.DEKORP-1A.001

Stiller, M., Kaerger, L., Agafonova, T., Krawczyk, C., Oncken, O., & Weber, M., & Former DEKORP Project Leaders, Former DEKORP Research Group, Former DEKORP Processing Centre. (2020b). Deep seismic reflection profile DEKORP 1987-1B across the western Rhenish Massif, West Germany. *GFZ Data Services*. [dataset]. https://doi.org/10.5880/GFZ.DEKORP-1B.001

Takei, Y. (2017). Effects of partial melting on seismic velocity and attenuation: A new insight from experiments. *Annual Review of Earth and Planetary Sciences*, *45*(1), 447–470. https://doi.org/10.1146/annurev-earth-063016-015820

Ueki, K., & Iwamori, H. (2016). Density and seismic velocity of hydrous melts under crustal and upper mantle conditions. *Geochemistry, Geophysics, Geosystems*, *17*(5), 1799–1814. https://doi.org/10.1002/2015GC006242

Van den Bogaard, P., & Schmincke, H.-U. (1985). Laacher see tephra—A widespread isochronous late quaternary tephra layer in central and northern Europe. *Geological Society of America Bulletin*, *96*(12), 1554–1571. https://doi.org/10.1130/0016-7606(1985)96%3C1554:LSTAWI%3E2.0.CO;2

Zöller, L., & Blanchard, H. (2009). The partial heat – Longest plateau technique: Testing TL dating of Middle and Upper Quaternary volcanic eruptions in the Eifel Area, Germany. *Quaternary Science Journal*, *58*(1), 86–106. https://doi.org/10.3285/eg.58.1.05

Zollo, A., Maercklin, N., Vassallo, M., Dello Iacono, D., Virieux, J., & Gasparini, P. (2008). Seismic reflections reveal a massive melt layer feeding Campi Flegrei caldera. *Geophysical Research Letters*, *35*(12), L12306. https://doi.org/10.1029/2008GL034242

References From the Supporting Information

Gonnermann, H. M., & Manga, M. (2013). Dynamics of magma ascent in the volcanic conduit. In S. A. Fagents, T. K. P. Gregg, & R. M. C. Lopes (Eds.), *Modeling volcanic processes: The physics and mathematics of volcanism* (pp. 55–84). Cambridge University Press.

Kaci, L. (2011). Strength and elasticity study of carbon dioxide (CO2) under high pressure. In *Digitized theses* (Vol. 3529). Retrieved from https://ir.lib.uwo.ca/digitizedtheses/3529

Kearey, P., Brooks, M., & Hill, I. (1991). *An introduction to geophysical prospecting*. Blackwell.

Kissling, E., Ellsworth, W. L., Eberhart-Phillips, D., & Kradolfer, U. (1994). Initial reference models in local earthquake tomography. *Journal of Geophysical Research*, *99*(B10), 19635–19646. https://doi.org/10.1029/93jb03138

Meissner, R. (1996). Faults and folds, fact and fiction. *Tectonophysics*, *264*(1–4), 279–293. https://doi.org/10.1016/s0040-1951(96)00132-1

Meissner, R., Bartelsen, H., & Murawski, H. (1981). Thin-skinned tectonics in the northern rhenish Massif, Germany. *Nature*, *290*(5805), 399–401. https://doi.org/10.1038/290399a0

Murawski, H. (1964). Die Nord-Süd-Zone der Eifel und ihre nördliche Fortsetzung. *Publ. Serv. Geol. Luxembourg*, *14*, 285–308.

NIST Chemistry WebBook. (2024). In P. J. Linstrom & W. G. Mallard (Eds.), *NIST chemistry WebBook, NIST standard reference database number 69*. National Institute of Standards and Technology. (retrieved October 8, 2024). https://doi.org/10.18434/T4D303

Schmitt, A. K., Klügel, A., Böddeker, S., Gothieu, M., & Gerdes, A. (2023). Depth and timing of magma evolution underneath the Emmelberg scoria cone in the West Eifel volcanic field. *Neues Jahrbuch für Mineralogie - Abhandlungen*, *198/2*(2), 101–118. https://doi.org/10.1127/njma/2023/0358

Shaw, C. S. J. (2004). The temporal evolution of three magmatic systems in the West Eifel volcanic field, Germany. *Journal of Volcanology and Geothermal Research*, *131*(3–4), 213–240. https://doi.org/10.1016/S0377-0273(03)00363-9

Shaw, C. S. J., Lebert, B. S., & Woodland, A. B. (2018). Thermodynamic modelling of mantle–melt interaction evidenced by veined wehrlite xenoliths from the Rockeskyllerkopf Volcanic Complex, West Eifel Volcanic Field, Germany. *Journal of Petrology*, *59*(1), 59–86. https://doi.org/10.1093/petrology/egy018

Witt-Eickschen, G. (2007). Thermal and geochemical evolution of the shallow subcontinental litho-spheric mantle beneath the Eifel: Constraints from mantle xenoliths, a review. In J. R. R. Ritter & U. R. Christensen (Eds.), *Mantle plumes - a multidisciplinary approach* (pp. 323–337). Springer.